

Genome-wide coexpression of steroid receptors in the mouse brain: Identifying signaling pathways and functionally coordinated regions

Ahmed Mahfouz^{a,b,1}, Boudewijn P. F. Lelieveldt^{a,b}, Aldo Grefhorst^c, Lisa T. C. M. van Weert^d, Isabel M. Mol^d, Hetty C. M. Sips^d, José K. van den Heuvel^d, Nicole A. Datson^{e,f}, Jenny A. Visser^c, Marcel J. T. Reinders^b, and Onno C. Meijer^d

^aDepartment of Radiology, Leiden University Medical Center, 2300 RC Leiden, The Netherlands; ^bDelft Bioinformatics Laboratory, Delft University of Technology, 2628 CD Delft, The Netherlands; ^cDepartment of Internal Medicine, Erasmus University Medical Center, 3000 CA Rotterdam, The Netherlands;

^dDivision of Endocrinology, Department of Internal Medicine, Leiden University Medical Center, 2300 RC Leiden, The Netherlands; ^eDivision of Medical Pharmacology, Leiden Academic Centre for Drug Research/Leiden University Medical Center, Leiden 2333 CC, The Netherlands; and ^fDepartment of Human Genetics, Leiden University Medical Center, Leiden 2300 RC, The Netherlands

Edited by Bruce S. McEwen, The Rockefeller University, New York, NY, and approved December 18, 2015 (received for review October 15, 2015)

Steroid receptors are pleiotropic transcription factors that coordinate adaptation to different physiological states. An important target organ is the brain, but even though their effects are well studied in specific regions, brain-wide steroid receptor targets and mediators remain largely unknown due to the complexity of the brain. Here, we tested the idea that novel aspects of steroid action can be identified through spatial correlation of steroid receptors with genome-wide mRNA expression across different regions in the mouse brain. First, we observed significant coexpression of six nuclear receptors (NRs) [androgen receptor (*Ar*), estrogen receptor alpha (*Esr1*), estrogen receptor beta (*Esr2*), glucocorticoid receptor (*Gr*), mineralocorticoid receptor (*Mr*), and progesterone receptor (*Pgr*)] with sets of steroid target genes that were identified in single brain regions. These coexpression relationships were also present in distinct other brain regions, suggestive of as yet unidentified coordinate regulation of brain regions by, for example, glucocorticoids and estrogens. Second, coexpression of a set of 62 known NR coregulators and the six steroid receptors in 12 non-overlapping mouse brain regions revealed selective downstream pathways, such as *Pak6* as a mediator for the effects of *Ar* and *Gr* on dopaminergic transmission. Third, *MageL2* and *Irs4* were identified and validated as strongly responsive targets to the estrogen diethylstilbestrol in the mouse hypothalamus. The brain- and genome-wide correlations of mRNA expression levels of six steroid receptors that we provide constitute a rich resource for further predictions and understanding of brain modulation by steroid hormones.

neuroendocrinology | nuclear receptors | transcription regulation | estrogens | glucocorticoids

Steroid receptors are part of the superfamily of nuclear receptors (NRs) that act as transcription factors regulating expression of numerous biologically important target genes (1). Their transcriptional activity is induced by steroid hormones, which respond to changed demands in terms of reproductive status, mineral balance, or stressful physical and psychological challenges. A crucial site of action is the brain, where these hormones have strong modulatory effects on physiological regulation, cognitive function, mood, and behavior. They do so by changing cellular responsiveness to a variety of neurotransmitters and peptides, and by inducing morphological changes (2, 3).

Understanding the effects of steroid hormones on the brain faces the challenge to identify in as many as 900 different brain nuclei (4) both the highly cell-specific target genes that mediate the hormone effects (5, 6) and the signaling factors that mediate or influence steroid receptor signaling. The latter include proteins affecting prereceptor metabolism, interacting transcription factors (7), and downstream NR coregulator proteins (1). Even if the effects of steroid hormones are well-studied in

specific regions (1, 8), overall, the brain steroid receptor targets and mediators remain largely unknown.

In situ hybridization (ISH) has been used to identify the functional roles of the 49 NR genes in adult mouse brain based on the clustering of the NR expression patterns in anatomical and regulatory networks (9). In this study, we substantially extended this approach to identify targets and signaling partners of the steroid receptors, and relationships between different regions of the mouse brain, based on genome-wide coexpression with steroid receptors. The Allen Brain Atlas (ABA) (4) is the most comprehensive repository of ISH-based gene expression in the adult mouse brain. We used the ABA to identify genes that have 3D spatial gene expression profiles similar to steroid receptors.

To validate the functional relevance of this approach, we analyzed the coexpression relationship of the glucocorticoid receptor (*Gr*) and estrogen receptor alpha (*Esr1*) and their known transcriptional targets in specific brain regions. We then exploited these associations to derive hypotheses about the functional role of receptors in brain regions with no previously known effects of steroids. Furthermore, we studied the region-specific coexpression of NRs and their downstream mediators (coregulators) to identify specific partners mediating the hormonal effects on dopaminergic transmission. Finally, to illustrate the potential of using spatial coexpression to predict region-specific steroid receptor targets

Significance

Steroid hormones coordinate the activity of many brain regions by binding to nuclear receptors that act as transcription factors. This study uses genome-wide correlation of gene expression in the mouse brain to discover (i) brain regions that respond in a similar manner to particular steroids, (ii) signaling pathways that are used in a steroid receptor and brain region-specific manner, and (iii) potential target genes and relationships between groups of target genes. The data constitute a rich repository for the research community to support further new insights in neuroendocrine relationships and to develop novel ways to manipulate brain activity in research or clinical settings.

Author contributions: A.M., B.P.F.L., M.J.T.R., and O.C.M. designed research; A.M., L.T.C.v.W., I.M.M., H.C.M.S., and J.K.v.d.H. performed research; A.G., N.A.D., and J.A.V. contributed new reagents/analytic tools; A.M. and L.T.C.v.W. analyzed data; and A.M., M.J.T.R., and O.C.M. wrote the paper.

The authors declare no conflict of interest.

This article is a PNAS Direct Submission.

Freely available online through the PNAS open access option.

See Commentary on page 2563.

¹To whom correspondence should be addressed. Email: a.mahfouz@lumc.nl.

This article contains supporting information online at www.pnas.org/lookup/suppl/doi:10.1073/pnas.1520376113/-DCSupplemental.

in the brain, we identified and validated genes that responded to changes in estrogen in the mouse hypothalamus (HY).

Results

Spatial Expression Reveals Known Sites of Action of Steroid Receptors in the Mouse Brain. We first analyzed the mRNA expression of six nuclear steroid receptors [*Esr1* and estrogen receptor beta (*Esr2*), androgen receptor (*Ar*), progesterone receptor (*Pgr*), *Gr*, and mineralocorticoid receptor (*Mr*)] across the brain using the 3D spatial gene expression data from the ABA (4). We generated a general overview of the expression of each receptor across 12 nonoverlapping brain structures covering the entire brain: isocortex; olfactory areas (OLF), hippocampal formation, cortical subplate, striatum (STR), pallidum (PAL), cerebellum, thalamus (TH), HY, midbrain (MB), pons, and medulla (Fig. 1A). The expression profiles generally correspond to the known distribution and sites of action of different receptors (9), and provide comprehensive information at the higher aggregation level of brain regions described here. For example, *Esr1* is highly expressed in the HY, OLF, and cortical subplate. Within the HY, *Esr1* shows high expression in the arcuate hypothalamic nucleus (ARH), and medial preoptic nucleus (MPO) (Fig. 1B). *Gr* is highly expressed in the cornu ammonis subdivision 1 (CA1) and dentate gyrus (DG) areas of the hippocampus, cortex, and TH, whereas *Mr* is predominantly expressed in the hippocampus (Fig. 1A). These expression patterns are well in line with the known sites of action of the different receptors across the brain (10, 11).

Genes Spatially Coexpressed with Steroid Receptors Indicate Regional Functional Specificity. To go beyond the expression profiles of steroid receptors as reported in the literature, we identified genes with similar expression profiles to each of the receptors. Based on the principle of “guilt by association,” these coexpressed genes are likely to be enriched in receptor target genes and receptor signaling partners such as coregulators. For each steroid receptor, we ranked genes based on their spatial coexpression across the whole brain as well as in each of the aforementioned 12 brain structures separately, resulting in 13 ranked lists per receptor (Dataset S1). (Datasets S1–S6 are available at data.3tu.nl/repository/uuid:ecc3b182-d312-4216-9053-a824d0e04d5e.) For each steroid receptor, strongly coexpressed genes within a brain region are likely related to the localized functional role of the receptor. For example, of the top 10 genes coexpressed with *Esr1* across the whole brain, four were previously shown to be regulated by ESR1 and/or estrogens in various tissues (*Gpr101*, *Calcr*, *Ngb*, and *Gpx3*) (12–15). These genes were also coexpressed with *Esr1* in the HY, in line with their functional relationship to *Esr1* in mediating, for example, reproductive and metabolic processes. However, whole-brain correlation of these genes with *Esr1* was also driven by the TH, MB, and PAL, demonstrating less obvious relationships between *Esr1* and these target genes. Strikingly, among the top 10 genes coexpressed with *Gr* across the whole brain, none are strongly coexpressed with *Gr* in the HY, indicating that *Gr* signaling in the HY is rather distinct from *Gr* signaling in the cortex, STR, TH, and MB.

In addition, we analyzed the functional enrichment of genes coexpressed with *Gr* and *Esr1* in the 12 brain regions (Table S1). *Esr1*-coexpressed genes were enriched for neuropeptide regulation in the HY as well as the cerebellum. A number of *Gr*-associated genes in the HY were related to glia and oligodendrocyte development, supporting the known effects of *Gr* on these processes in the HY (16).

Glucocorticoid-Responsive Genes Are Highly Expressed with *Gr* in HP, Pons, MB, and Whole Brain. To test the validity of our hypothesis that coexpressed genes constitute candidate targets of steroid receptors, we assessed the extent of coexpression between *Gr* and known GR target genes. Because *Gr* has an important role in mediating transcription of genes involved in coping with stress within the hippocampus (2), we analyzed the coexpression of glucocorticoid (GC)-responsive genes (i.e., likely GR targets) with *Gr* in the whole brain and hippocampus, and in its

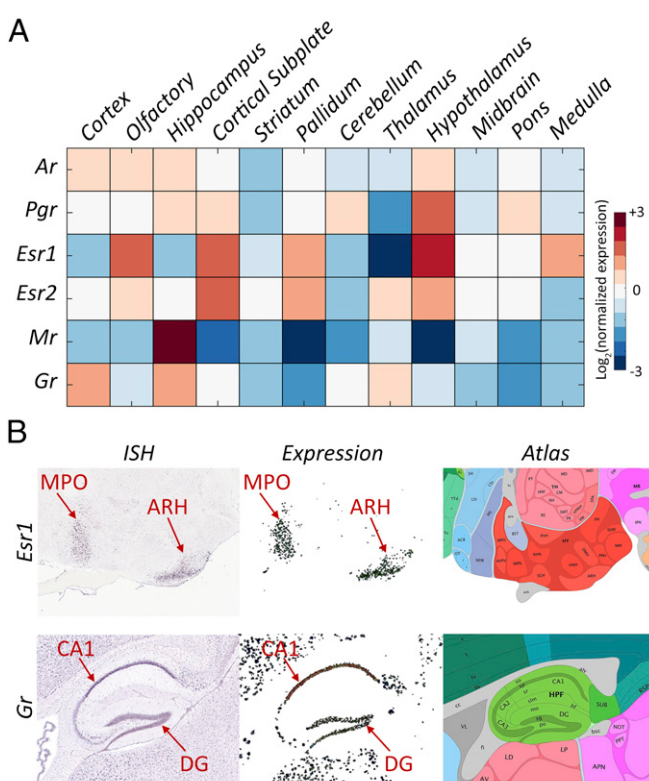


Fig. 1. Expression of steroid receptors in the mouse brain. (A) Expression of six steroid receptors across the 12 brain regions. Reported values are the average expression energy per region normalized to the average expression across the whole brain and then \log_2 -transformed. (B) Example sagittal sections from the Allen Brain Atlas (4) showing the ISH (Left), expression mask (Middle), and corresponding atlas section (Right) of *Esr1* in the HY (Top) and *Gr* in the hippocampus (Bottom). Red arrows indicate the MPO, ARH, CA1, and DG.

substructures, such as the DG and the different subregions of the CA (Fig. 2A and Dataset S2). The set of GC-responsive genes we considered originates from experiments where male rats were exposed to GC treatment in a chronic restraint stress (CRS) condition as well as in a control situation (17). These experiments resulted in three sets of genes differentially expressed in DG neurons: (i) GC-responsive genes in CRS rats, (ii) GC-responsive genes in control rats, and (iii) genes that show differential expression in GC treatment for both conditions (common GC-responsive genes).

As expected, GC-responsive genes are significantly coexpressed with *Gr* in the DG (where they were identified) but, interestingly, also in the whole brain and in the CA3 region [false discovery rate (FDR)-corrected $P < 1.8 \times 10^{-3}$; Mann–Whitney *U* test]. The significant coexpression of GC-responsive genes in the CA3 area indicates that those cells in CA3 that do express *Gr* (10) may be functionally linked to DG granule cells in terms of their response to GCs. Of note, only those genes that responded to GC treatment in stressed and control rats (common GC-responsive genes) showed a significant coexpression with *Gr* in the DG, CA1, and (very substantially) CA3 regions of the hippocampus. The data reveal that only the subset of invariant, context-independent GR target genes is related to constitutive coexpression with *Gr*, even if the correlation data come from “control” conditions.

The coexpression of the GC-responsive gene sets with *Gr* was not significant for areas such as the HY and the cortex. We initially considered these negative control regions, given that the target genes were identified in microdissected DG granule neurons (17) and the presumed high degree of cell specificity. However, the coexpression of *Gr* with GC-responsive genes in CA3 prompted us to test whether this coexpression also occurs in other brain areas. Fig. 2B shows that the set of common GC-responsive genes is not only coexpressed with

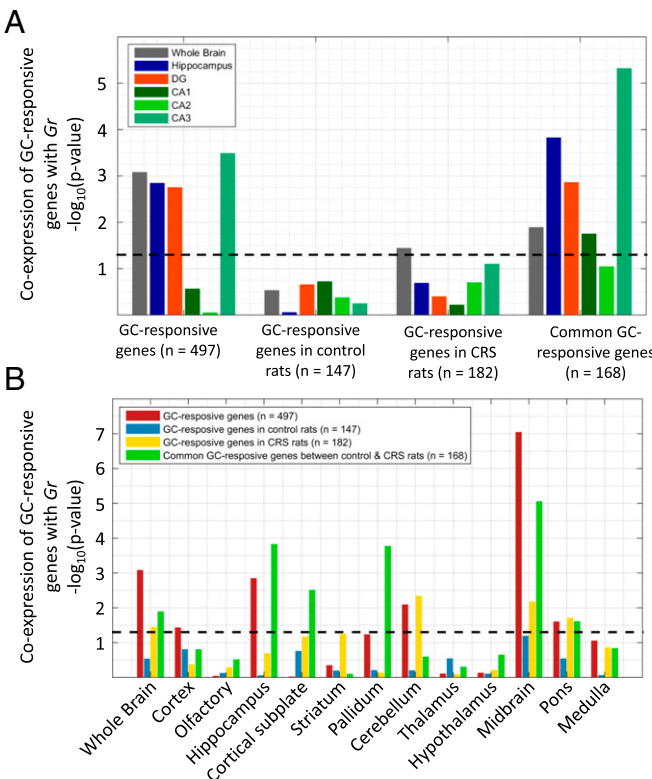


Fig. 2. Coexpression of GC-responsive genes and *Gr* in the hippocampus. (A) Coexpression of four GC-responsive gene sets with *Gr* in the whole brain, hippocampus, DG, CA1, CA2, and CA3. (B) Coexpression of four GC-responsive gene sets with *Gr* across the whole brain, as well as the 12 major brain structures. All bars indicate the $-\log_{10}$ of the Wilcoxon rank sum test, and the dashed line indicates the significance level at $P = 0.05$.

Gr in the hippocampus (DG, CA1, and CA3) but also in the cortical subplate, PAL, and MB. These associations indicate a potential, as yet unknown, relationship between these three brain areas in terms of endocrine regulation, in accordance with the notion that the cellular responses to GCs can be similar in distributed parts of brain networks (18). Taken together, these results show that GR targets are coexpressed with *Gr* in the DG, the region where responsiveness was measured, as well as pointing to other brain regions that might share the same regulation mechanism.

Sexually Dimorphic Genes Are Highly Coexpressed with *Esr1* in the HY. To illustrate the generalizability of our approach to other receptors and brain regions, we followed the same approach to analyze the coexpression of *Esr1* and its putative targets. Xu et al. (19) showed that a set of 16 genes, including *Esr1*, has sexual dimorphic expression in the adult mouse HY. In addition, they showed that these 16 genes are sensitive to gonadal steroids (also in the male mouse brain) and that some are necessary for effects of estrogens on sexually dimorphic behavior (19), making this set of ESR1 targets in the HY quite valuable.

Table S2 shows the correlation values for each of the 15 sexually dimorphic genes with *Esr1* in whole brain, as well as in the HY, based on data from the ABA. The set of 15 genes is significantly correlated to *Esr1* based on whole-brain analysis (FDR-corrected $P = 8.69 \times 10^{-14}$, Mann–Whitney U test) as well as the hypothalamic expression pattern ($P = 3.85 \times 10^{-10}$). To test whether the correlation between the 15 genes and *Esr1* is HY-specific, we repeated the analysis for all 12 brain structures. Fig. 3A shows that sexually dimorphic genes are mostly correlated to *Esr1* in the HY, PAL, TH, and STR ($P < 10^{-6}$). Similar to the results obtained for GR target genes, we observed high coexpression outside the main region of action (e.g., in the PAL), suggesting that these brain regions share aspects of their

transcriptional response to estrogen receptor activation. Furthermore, sex steroid receptors (*Esr1*, *Esr2*, and *Pgr*) showed higher coexpression levels with the sexually dimorphic genes with respect to the stress steroid-related *Mr* and *Gr* in the HY (Fig. 3B). The strongest coexpression was with *Esr1*, indicating that the hypothalamic sexual dimorphism genes are mainly, but probably not exclusively, related to *Esr1*. Taken together, these results show that spatial coexpression can pinpoint context-specific actions of steroid receptors (in this case, *Gr* and *Esr1*) and yields region-specific coexpressed genes, a very rich resource with which to generate hypotheses about steroid receptor targets.

Region-Specific Coregulator Analysis Points to Dopaminergic Transmission via *Pak6*.

So far, we have analyzed the potential of genes coexpressed with receptors to include region-specific targets. However, because correlation only indicates association rather than causation, coexpressed genes can also include coregulators of steroid receptors. Previous studies have shown the signaling pathways of steroid receptors to differ across brain regions in a gene-specific manner (1, 20). To identify putative region-dependent coregulators of steroid receptors, we analyzed the coexpression relationships of each steroid receptor and a set of 62 NR coregulators as present on a peptide array (21) (complete data are provided in Dataset S3). Fig. 4A shows that the expression of coregulators varies greatly across the different brain regions. For example, although *Ncoa1* is expressed in a fairly homogeneous manner, conforming to earlier results (20), *Ncoa4* is substantially enriched in the caudal brain regions.

The coexpressions of coregulators with the *Ar*, *Gr*, and *Mr* differ greatly across different brain regions, indicating selective coregulation (Fig. 4B–D). For example, the AR/GR coactivators *Pias2* (22) and *Ncoa4* (23) are highly coexpressed with *Gr* in the MB and HY, respectively (Fig. 4C). However, both coactivators are not coexpressed with *Ar* within the same regions even though the relative abundance of *Ar* in the MB and the HY is higher than *Gr* (Fig. 1A). *Mr* is predominantly expressed in the

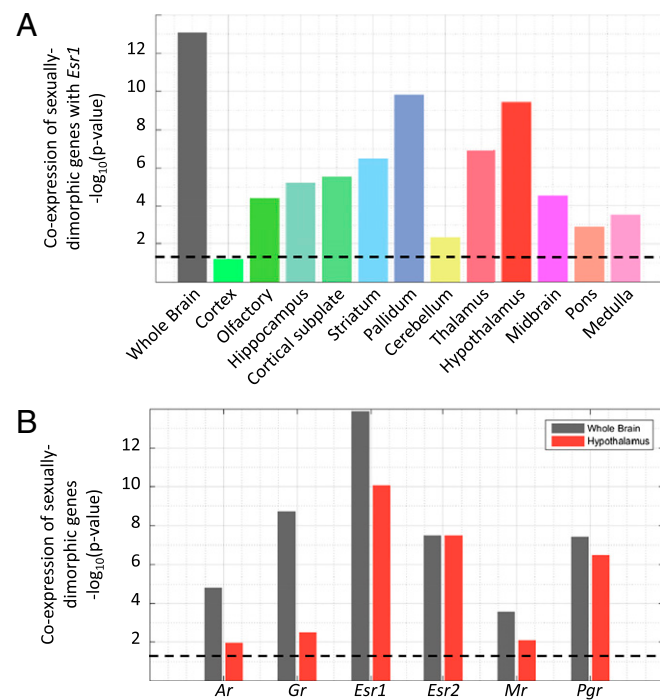


Fig. 3. Coexpression of sexually dimorphic genes and *Esr1* in the HY. (A) Coexpression of 15 sexually dimorphic genes with *Esr1* across the mouse brain. (B) Coexpression of the 15 sexually dimorphic genes with the six steroid receptors across the whole brain, as well as the HY. All bars indicate the $-\log_{10}$ of the Wilcoxon rank sum test, and the dashed line indicates the significance level at $P = 0.05$.

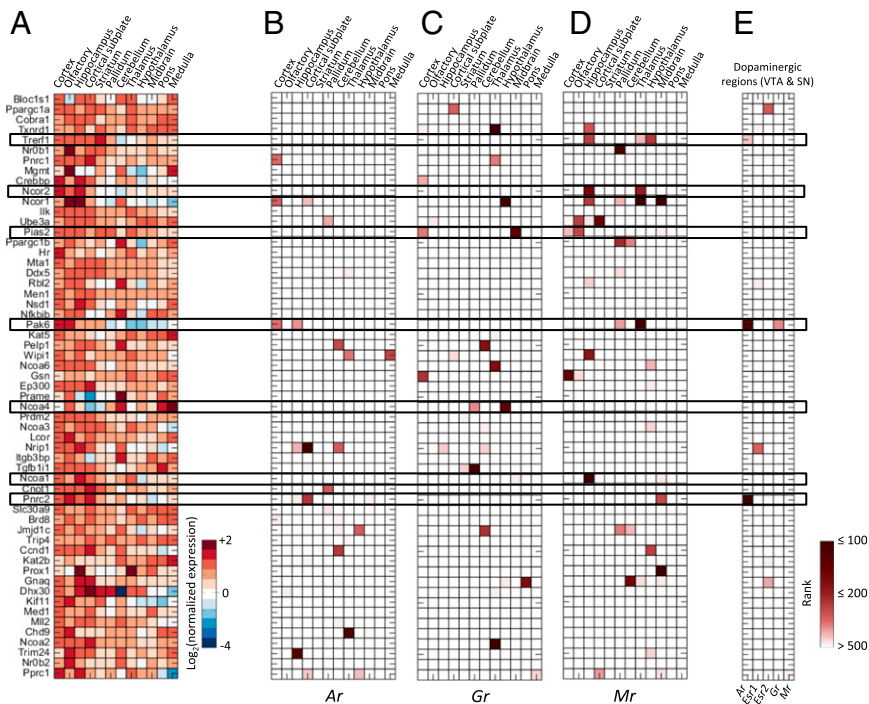


Fig. 4. Coexpression of coregulators and steroid receptors. (A) Expression of 62 coregulators in 12 brain regions. Reported values are the average expression energy per region normalized to the average expression across the whole brain and then log₂-transformed. Coexpression ranks of the 62 coregulators with *Ar* (B), *Gr* (C), and *Mr* (D). Dark red corresponds to high rank (i.e., strong coexpression). (E) Rank sum of the coexpression rank of each coregulator with *Ar* in the dopaminergic regions (VTA and SN).

hippocampus, where it is highly coexpressed with *Ncoa1*, *Txnr1*, *Trefl*, *Ncor1*, *Wip1*, and *Ncor2* (Fig. 4D). Although *Ncoa1* is a known MR coregulator (24), little is known about the effect of the other coregulators on MR function in the hippocampus, and they might be good candidates for further functional analysis.

Because there still is substantial heterogeneity across the 12 brain regions that we initially analyzed, we narrowed down our analysis to well-established target regions of steroid hormone action. We analyzed the coexpression of the 62 coregulators with the steroid receptors in dopaminergic regions in the ventral tegmental area (VTA) and substantia nigra (SN), which are known targets of steroid actions (25, 26) (Figs. S1 and S2). We found three significantly coexpressed coregulators with *Ar* in VTA/SN: *Pnrc2*, *Pak6*, and *Trefl* (Fig. 4E and Dataset S4), suggesting that these coregulators may be involved in mediating AR effects on dopaminergic transmission. Furthermore, only *Pak6* was strongly coexpressed with *Gr* in the dopaminergic regions ($P < 0.01$). Thus, AR and GR may share some, but not all, coregulators, much like the fact that AR binding sites may overlap, in part, with GR binding sites (27). These results indicate that we can use genome-wide spatial coexpression not only to analyze the relationship between the receptors and their targets but also to identify region-specific coregulators.

Predictive Value of Coexpression for Hormone Responsiveness: *MageL2*

Is Likely a Target of ESR1. Finally, we set out to test the predictive value of high coexpression with a steroid receptor to identify transcriptional targets. We measured the response of genes that are highly coexpressed with *Esr1* in the HY to estrogen diethylstilbestrol (DES) in castrated male mice using quantitative PCR (qPCR) (*SI Materials and Methods*). In the male brain, testosterone can be metabolized to estrogen or act directly via the AR. To avoid interpretation difficulties, we decided to activate brain estrogen receptors directly with the selective ligand DES. We selected the top 10 most strongly coexpressed genes with *Esr1* in the HY. As a negative control, we used the set of genes that are not coexpressed with *Esr1* in the HY. Fig. 5A shows examples, from the ISH experiments of the ABA, of *Irs4* and *Magel2*, two of the strongly coexpressed genes selected for validation. Because *Esr1* is not homogeneously expressed across the HY (Fig. 1B), we analyzed the responsiveness of the set of top 10 genes to DES in the anterior (MPO) and posterior (ARH) parts of the HY separately. Fold-change up-regulation was modest,

which may be due to nonresponsiveness, a modest transcriptional response of brain targets, or dilution of the signal in the hypothalamic homogenates (**Table S3**).

To confirm colocalization further, we performed quantitative double ISH (dISH) for *Esr1* and the six mRNAs (*Irs4*, *Magel2*, *Adck4*, *Unc5*, *Ngb*, and *Gdpd2*) that showed more than 1.3-fold enrichment in qPCR. *Esr1* mRNA was consistently down-regulated more than twofold upon DES treatment, validating the treatment (Fig. S3). *Irs4* and *Magel2* mRNA were both significantly up-regulated by DES treatment in MPO (1.9-fold and 2.4-fold, respectively), whereas only *Magel2* was up-regulated in ARH (2.6-fold) (Fig. 5 B and D). A 1.3-fold induction of *Ngb* mRNA in ARH did not reach statistical significance, whereas *Gdpd2*, *Unc5d*, and *Adck4* mRNA levels showed no trend of regulation after DES treatment (Fig. S4).

The data indicate that additional criteria are necessary for reliable target prediction. Because *Irs4* and *Magel2* are among the top genes expressed in the HY (ranked 1 and 11, respectively) compared with a ranking of 141 for *Adck4* and 284 for *Unc5d*, these criteria may include a combination of expression, coexpression filters, and other criteria.

Identifying GR-Related Corticosterone Targets in the Hippocampus.

Using gene expression measurements (qPCR and dISH), we validated the responsiveness of *Irs4* and *Magel2* as predicted ESR1 targets to DES treatment. Despite its importance, especially in detecting colocalization, gene expression remains an indirect measurement of interaction. Therefore, we set out to detect genomic binding of steroid receptors directly using chromatin immunoprecipitation followed by next-generation sequencing (ChIP-Seq). Previously, we used ChIP-Seq to identify genomic binding sites of GR in the rat hippocampus (28). Reanalyzing this data, we identified 694 corticosterone target genes with GR binding sites, of which 16 were within the top 200 genes coexpressed with *Gr* in the hippocampus (16 of 200; $P = 9.97 \times 10^{-5}$, one-sided Fisher's exact test; Table S4). Fig. S5 shows examples of the GR binding sites we identified in genes strongly coexpressed with *Gr*. We did not observe any significant enrichment of corticosterone target genes in the 200 genes with the lowest correlation to *Gr* in the hippocampus (five of 200; $P = 0.62$, one-sided Fisher's exact test) or in the set of 200 genes with the highest correlation to *Esr1* in the hippocampus (one of 200; $P = 1$, one-sided Fisher's exact test).

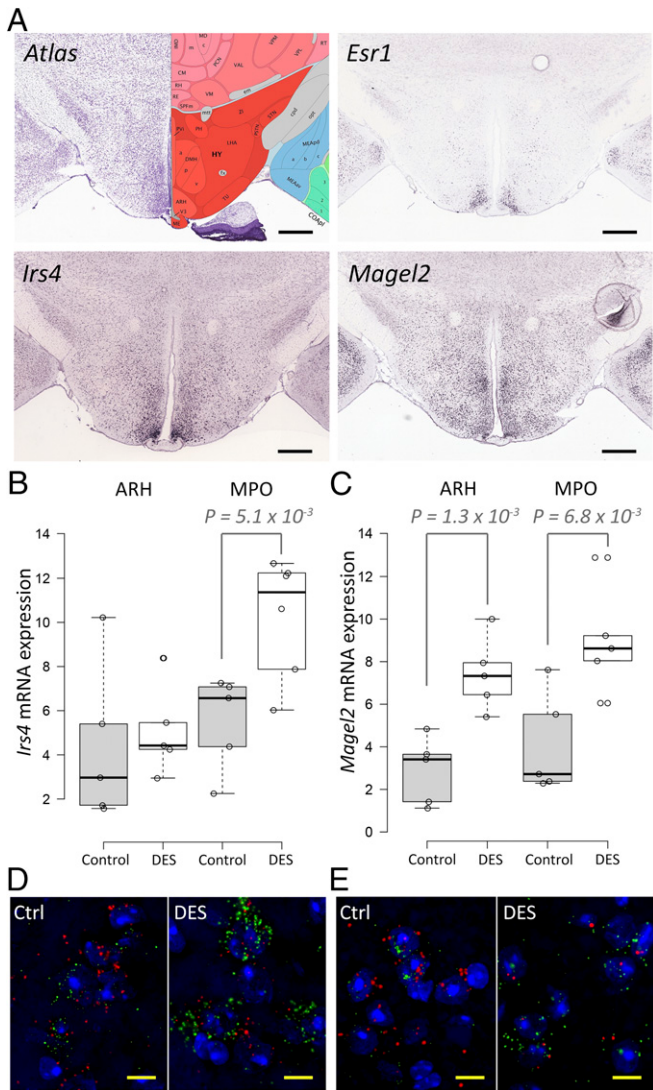


Fig. 5. Highly coexpressed genes are potential steroid targets. (A) Coronal ISH sections showing the expression of *Esr1*, *Irs4*, and *Magel2*. (Scale bars, 600 μ m.) Data taken from the Allen Brain Atlas (4). Response of *Irs4* (B) and *Magel2* (C) to DES treatment in castrated mice in the MPO and ARH using dISH. (D) dISH of *Esr1* (red) and *Irs4* (green) in the anterior HY. (Scale bars, 10 μ m. Magnification, 100 \times .) (E) dISH of *Esr1* (red) and *Magel2* (green) in the anterior HY. (Scale bars, 10 μ m. Magnification, 100 \times .) mRNA expression in ISH was quantified as the percentage of the image surface with positive signal. Reported *P* values are calculated with a one-sided, two-sample *t* test with a significant level at *P* < 0.05.

Discussion

Because nuclear steroid receptors act as transcription factors, they may be expected a priori to coexpress with their target genes and signaling partners. In the brain, the effects of steroid receptors are region-specific, and by analyzing their spatial coexpression relationships across different brain regions, we can define potential targets and partners, as well as parallels between brain areas. The complexity and large variability in gene expression across the brain have forced many studies to analyze either brain-wide expression of a small set of genes or genome-wide expression in a few regions. The availability of high-resolution ISH-based expression maps of the mouse brain in the ABA allows the identification of all genes with a similar expression pattern across many brain regions that might indicate functional similarity between the gene products (29). We provide a comprehensive description of the coexpression of genes with six receptors of gonadal and adrenal steroid hormones in the male mouse brain. Our

results demonstrate that genes that are spatially coexpressed with receptors in a region-specific manner can enhance our understanding of brain modulation by steroid hormones.

Using genome-wide spatial coexpression analysis, we observed strong coexpression of known GR transcriptional targets in the hippocampus and known ESR1 transcriptional targets in the HY. These observations support our hypothesis that genes showing strong coexpression with a steroid receptor are enriched in transcriptional targets and/or coregulators of that receptor. In addition, the unanticipated coexpression of genes with these receptors outside their known sites of action may extend our understanding of the coordinated steroid response of the brain. For example, the high coexpression between *Gr* and its GC-responsive target genes (originally derived from the DG) in CA3, the MB, and the PAL is in line with a network that has been referred to as the neurocircuitry of stress (30). Likewise, dendritic complexity of neurons and excitability are modulated by GCs and stress across different brain regions simultaneously (18). Such similar responses of distinct brain regions suggest similar cellular machinery, and thus similarly correlated gene expression with the responsible receptor.

For the genes that are expressed in a sex-specific manner, we confirmed their coexpression with *Esr1*, *Esr2*, and *Pgr*, which is in accordance with their regulation by gonadal steroids (19). Lack of coexpression with *Ar* may reflect the fact that many testosterone effects on the HY are mediated by estrogen receptors after aromatization of testosterone into estradiol. It is as yet unclear whether the significant coexpression with *Pgr* reflects simply coexpression of *Esr1* and *Pgr* or also points to progesterone regulation of these genes. Regardless, we extended the coexpression between sexually dimorphic genes to extrahypothalamic sites, pointing to a parallel regulation in, at least, the PAL, a region that includes the bed nucleus of the stria terminalis, where regulation by (nonspecified) gonadal hormones has been observed (19).

Our analysis of the coexpression of coregulators and steroid receptors identified known relationships, such as the high coexpression between *Ncoa1* and *Mr* in the hippocampus (20). More importantly, this brain-wide analysis provides an overview of potentially unknown relationships between steroid receptors and coregulators. By focusing on dopaminergic regions (VTA and SN), we identified strong coexpression of *Pak6* with *Ar* as well as *Gr*. Of interest, *Pak6* is a known AR coregulator (31) and *Pak6* KO mice show several locomotion and behavioral deficits that are likely related to disturbed dopaminergic transmission (32). Thus, this example of *Pak6* coexpression underscores the feasibility of our methodology to find potential partners of nuclear steroid receptors. Of note, steroid receptor/coactivator interactions may be induced with a certain degree of specificity by selective modulator types of steroid receptor ligands (24, 33). The coexpression of steroid receptors with their coactivators may not only predict steroid responsiveness but also point to selective activation of particular circuits with synthetic ligands (24).

To test whether spatial coexpression can be used to predict transcriptional targets of steroid receptors in the brain, we used qPCR and dISH to assess if genes strongly coexpressed with *Esr1* in the HY include any ESR1 targets. Among the tested genes we identified two estrogen-regulated genes: *Irs4*, a previously known ESR1 target (19); and *Magel2*, a previously unidentified ESR1 target. Loss of *Magel2* leads to impaired reproduction, providing an immediate link to estrogen regulation (34). This gene is deleted in Prader–Willi syndrome, which is associated with hypogonadotropic hypogonadism, obesity, and hyperphagia (35). Likewise, *Irs4* has a role in hypothalamic leptin signaling and regulation of metabolism (36). Therefore, hypothalamic estrogen responsiveness of *Magel2* and *Irs4* may be related to estrogen effects on metabolism (37). The presently modest predictive power may be improved by incorporating the effect size (i.e., the absolute expression of a gene), given the values for true positives *Irs4* and *Magel2*. Also, the presence of conserved steroid response elements on the DNA could be a useful additional filter (38).

The enrichment of known targets and coregulators of a certain NR within the same brain regions where the NR is

expressed confirms the validity of our analysis. Our approach is even strengthened by the notion that the receptor and its targets and/or coregulators are significantly coexpressed despite the genome-wide and brain-wide qualitative approach of measuring mRNA levels using ISH. However, there are some intrinsic limitations to the analysis. First, although the quality of ISH is overall high, it is insufficient for some genes. Of the three datasets covering expression of *Gr*, only one was of sufficient quality. Also, *Ncoa1*, which codes for an important coregulator for ESR1 and GR (1, 20), is expressed at low levels and not significantly associated with the two receptors. Consequently, there is the risk for increased false-negative results associated with a genome-wide approach using these data. Second, the ABA maps the expression of all genes under the same normal conditions. This dataset, although unique in its brain-wide and genome-wide coverage, does not include variations between individuals or context-specific expression patterns (*SI Materials and Methods*).

Our approach relies on Pearson's correlation as a measure of similarity between 3D expression patterns of genes, summarized to 200- μ m isotropic voxels. Although using the expression volumes instead of the original ISH slices simplifies computations and reduces noise effects, the lower resolution yields the analysis of small brain nuclei unreliable. For example, the very small number of voxels representing dorsal raphe nucleus in the 3D atlas hampered analysis of the serotonergic dorsal raphe nucleus. By using

- Stanisić V, Lonard DM, O'Malley BW (2010) Modulation of steroid hormone receptor activity. *Prog Brain Res* 181:153–176.
- de Kloet ER, Joëls M, Holsboer F (2005) Stress and the brain: From adaptation to disease. *Nat Rev Neurosci* 6(6):463–475.
- Toffoletto S, Lanzenberger R, Gingell M, Sundström-Poromaa I, Comasco E (2014) Emotional and cognitive functional imaging of estrogen and progesterone effects in the female human brain: A systematic review. *Psychoneuroendocrinology* 50:28–52.
- Lein ES, et al. (2007) Genome-wide atlas of gene expression in the adult mouse brain. *Nature* 445(7124):168–176.
- John S, et al. (2011) Chromatin accessibility pre-determines glucocorticoid receptor binding patterns. *Nat Genet* 43(3):264–268.
- Krum SA, et al. (2008) Unique ERalpha cistromes control cell type-specific gene regulation. *Mol Endocrinol* 22(11):2393–2406.
- Ravasi T, et al. (2010) An atlas of combinatorial transcriptional regulation in mouse and man. *Cell* 140(5):744–752.
- Datson NA, et al. (2012) The transcriptional response to chronic stress and glucocorticoid receptor blockade in the hippocampal dentate gyrus. *Hippocampus* 22(2):359–371.
- Gofflot F, et al. (2007) Systematic gene expression mapping clusters nuclear receptors according to their function in the brain. *Cell* 131(2):405–418.
- Reul JMHM, de Kloet ER (1985) Two receptor systems for corticosterone in rat brain: microdistribution and differential occupation. *Endocrinology* 117(6):2505–2511.
- Pérez SE, Chen E-Y, Mufson EJ (2003) Distribution of estrogen receptor alpha and beta immunoreactive profiles in the postnatal rat brain. *Brain Res Dev Brain Res* 145(1):117–139.
- Nilaweera KN, et al. (2008) G protein-coupled receptor 101 mRNA expression in supraoptic and paraventricular nuclei in rat hypothalamus is altered by pregnancy and lactation. *Brain Res* 1193:76–83.
- Kanno S, Hirano S, Kayama F (2004) Effects of the phytoestrogen coumestrol on RANK-ligand-induced differentiation of osteoclasts. *Toxicology* 203(1–3):211–220.
- De Marinis E, et al. (2013) 17 β -Oestradiol anti-inflammatory effects in primary astrocytes require oestrogen receptor β -mediated neuroglobin up-regulation. *J Neuroendocrinol* 25(3):260–270.
- Baltgalvis KA, Greising SM, Warren GL, Lowe DA (2010) Estrogen regulates estrogen receptors and antioxidant gene expression in mouse skeletal muscle. *PLoS One* 5(4):e10164.
- Zia MTK, et al. (2015) Postnatal glucocorticoid-induced hypomyelination, gliosis, and neurologic deficits are dose-dependent, preparation-specific, and reversible. *Exp Neurol* 263:200–213.
- Datson NA, et al. (2013) Previous history of chronic stress changes the transcriptional response to glucocorticoid challenge in the dentate gyrus region of the male rat hippocampus. *Endocrinology* 154(9):3261–3272.
- Dias-Ferreira E, et al. (2009) Chronic stress causes frontostriatal reorganization and affects decision-making. *Science* 325(5940):621–625.
- Xu X, et al. (2012) Modular genetic control of sexually dimorphic behaviors. *Cell* 148(3):596–607.
- Lachize S, et al. (2009) Steroid receptor coactivator-1 is necessary for regulation of corticotropin-releasing hormone by chronic stress and glucocorticoids. *Proc Natl Acad Sci USA* 106(19):8038–8042.
- Nwachukwu JC, et al. (2014) Resveratrol modulates the inflammatory response via an estrogen receptor-signal integration network. *Elife* 2014(3), 10.7554/Elife.02057.
- Kotaja N, Aittomäki S, Silvennoinen O, Palvimo JJ, Jänne OA (2000) ARIP3 (androgen receptor-interacting protein 3) and other PIAS (protein inhibitor of activated STAT) proteins differ in their ability to modulate steroid receptor-dependent transcriptional activation. *Mol Endocrinol* 14(12):1986–2000.
- Alen P, et al. (1999) Interaction of the putative androgen receptor-specific coactivator ARA70/ELE1alpha with multiple steroid receptors and identification of an internally deleted ELE1beta isoform. *Mol Endocrinol* 13(1):117–128.
- Zalachoras I, et al. (2013) Differential targeting of brain stress circuits with a selective glucocorticoid receptor modulator. *Proc Natl Acad Sci USA* 110(19):7910–7915.
- Niwa M, et al. (2013) Adolescent stress-induced epigenetic control of dopaminergic neurons via glucocorticoids. *Science* 339(6117):335–339.
- Purves-Tyson TD, et al. (2014) Testosterone induces molecular changes in dopamine signaling pathway molecules in the adolescent male rat nigrostriatal pathway. *PLoS One* 9(3):e91151.
- Schauwaerts K, et al. (2007) Loss of androgen receptor binding to selective androgen response elements causes a reproductive phenotype in a knockin mouse model. *Proc Natl Acad Sci USA* 104(12):4961–4966.
- Polman JA, de Kloet ER, Datson NA (2013) Two populations of glucocorticoid receptor-binding sites in the male rat hippocampal genome. *Endocrinology* 154(5):1832–1844.
- Dong H-W, Swanson LW, Chen L, Fanselow MS, Toga AW (2009) Genomic-anatomic evidence for distinct functional domains in hippocampal field CA1. *Proc Natl Acad Sci USA* 106(28):11794–11799.
- Shin LM, Liberzon I (2010) The neurocircuitry of fear, stress, and anxiety disorders. *Neuropsychopharmacology* 35(1):169–191.
- Lee SR, et al. (2002) AR and ER interaction with a p21-activated kinase (PAK6). *Mol Endocrinol* 16(1):85–99.
- Nekrasova T, Jobes ML, Ting JH, Wagner GC, Minden A (2008) Targeted disruption of the Pak5 and Pak6 genes in mice leads to deficits in learning and locomotion. *Dev Biol* 322(1):95–108.
- Atucha E, et al. (2015) A mixed glucocorticoid/mineralocorticoid selective modulator with dominant antagonism in the male rat brain. *Endocrinology* 156(11):4105–4114.
- Mercer RE, Wevrick R (2009) Loss of magel2, a candidate gene for features of Prader-Willi syndrome, impairs reproductive function in mice. *PLoS One* 4(1):e4291.
- Eiholzer U, et al. (2006) Hypothalamic and gonadal components of hypogonadism in boys with Prader-Labhart-Willi syndrome. *J Clin Endocrinol Metab* 91(3):892–898.
- Sadagurski M, Dong XC, Myers MG, Jr, White MF (2014) Irs2 and Irs4 synergize in non-LepRb neurons to control energy balance and glucose homeostasis. *Mol Metab* 3(1):55–63.
- Frank A, Brown LM, Clegg DJ (2014) The role of hypothalamic estrogen receptors in metabolic regulation. *Front Neuroendocrinol* 35(4):550–557.
- Datson NA, et al. (2011) Specific regulatory motifs predict glucocorticoid responsiveness of hippocampal gene expression. *Endocrinology* 152(10):3749–3757.
- Ng L, et al. (2007) Neuroinformatics for genome-wide 3D gene expression mapping in the mouse brain. *IEEE/ACM Trans Comput Biol Bioinformatics* 4(3):382–393.
- Chen EY, et al. (2013) Enrichr: Interactive and collaborative HTML5 gene list enrichment analysis tool. *BMC Bioinformatics* 14(1):128.
- Benjamini Y, Hochberg Y (1995) Controlling the false discovery rate: A practical and powerful approach to multiple testing. *J R Stat Soc Series B Stat Methodol* 57(1):289–300.
- Datson NA, et al. (2009) A molecular blueprint of gene expression in hippocampal subregions CA1, CA3, and DG is conserved in the brain of the common marmoset. *Hippocampus* 19(8):739–752.
- Boon MR, et al. (2014) Peripheral cannabinoid 1 receptor blockade activates brown adipose tissue and diminishes dyslipidemia and obesity. *FASEB J* 28(12):5361–5375.
- Li H, Durbin R (2009) Fast and accurate short read alignment with Burrows-Wheeler transform. *Bioinformatics* 25(14):1754–1760.
- Zhang Y, et al. (2008) Model-based analysis of ChIP-Seq (MACS). *Genome Biol* 9(9):R137.
- Robinson JT, et al. (2011) Integrative genomics viewer. *Nat Biotechnol* 29(1):24–26.

Supporting Information

Mahfouz et al. 10.1073/pnas.1520376113

SI Materials and Methods

Allen Mouse Brain Atlas. The ABA of the Mouse Brain (4) (mouse.brain-map.org) is a spatially mapped ISH gene expression atlas of the 8-wk-old adult C57BL/6J male mouse brain. The genome-wide atlas contains expression data for ~20,000 genes. For each gene, ISH brain sections were sampled at 25- μ m intervals across the entire brain. The high (in-plane)-resolution primary data from each experiment were reconstructed in three dimensions and registered to the Nissl stain-based reference atlas [Allen Mouse Reference Atlas (ARA)], created specifically for this project. For each gene, the data were then aggregated into isotropic voxels defined by a uniform 200- μ m grid in the reference space. Resulting data consist of a spatially aligned 67 \times 41 \times 58 (rostral-caudal, dorsal-ventral, left-right) volume for each gene. The ontology of the ARA is used to label individual voxels with their anatomical nomenclature. Some genes were assayed more than once, using a different probe or plane of sectioning (sagittal or coronal). Generally, ~20,000 genes were assayed using sagittal-sectioning experiments, whereas the coronal-sectioning experiments were carried out for ~4,000 genes.

The Allen Mouse Brain Atlas provides expression of genes under normal conditions. Brain sections were collected from thousands of animals, and hence do not represent a single individual. In brief, each brain sectioned in either the sagittal or coronal plane was used to generate eight series (each series contains five slides, each slide contains four sections) (4). Each of these series was hybridized to a single gene with each physical brain used to survey several independent genes (39). For many genes in the dataset, several experiments were conducted, resulting in multiple measurements of those genes from different animals. Moreover, for genes assayed using both sagittal and coronal sectioning experiments, sections were collected from different animals. A visual analysis of the expression pattern of the *Man1a* gene which is measured using 19 different experiments (18 sagittal and 1 coronal) shows a high consistency of expression patterns, although these patterns come from different animals.

Data Preprocessing. We downloaded the 26,069 expression energy volumes corresponding to all experiments (21,722 sagittal and 4,347 coronal) through the Application Programming Interface of the ABA on February 12, 2013. Expression energy, $E(S)$, is a measurement combining the expression level [$I(v)$; the integrated amount of signal within each voxel] and the expression density (the amount of “expressing cells” within each voxel). The average expression energy of gene g in region S is calculated as:

$$E_g(S) = \frac{\sum_{v \in S} M(v) \times I(v)}{|S|},$$

where v is a voxel in region S , $|S|$ is the total number of voxels representing S , and $M(v)$ is a binary expression mask with 1’s and 0’s representing expressing and nonexpressing voxels, respectively.

In sagittal-sectioning experiments, data were generated from the left hemisphere of the brain only while in coronal-sectioning experiments; data were generated from both hemispheres. Voxels with more than 20% missing data (no gene expression value) were removed from further analysis, resulting in 27,365 voxels in the sagittal datasets and 61,164 voxels in the coronal datasets.

Spatial Coexpression. We used Pearson’s correlation coefficient as a measure of similarity between 3D spatial expression profiles. Given a steroid receptor of interest (seed gene), we calculate the

Pearson’s correlation between the spatial expression profile of that seed gene and every other gene in the ABA based on the expression values within any structure of interest (e.g., for the whole brain, correlations were calculated based on the expression across 27,365 voxels in the sagittal datasets and 61,164 voxels in the coronal dataset).

Together with the coexpression calculations, we also calculated the average expression energy of gene g in structure S , $E_g(S)$, as well as the normalized average expression $K_g(S)$:

$$K_g(S) = \frac{E_g(S)}{E_g(\text{Brain})},$$

where $E_g(\text{Brain})$ is the average expression of gene g in the whole-mouse brain.

Enrichment Analysis. To characterize the functional associations of NRs in each of the 12 brain regions, we performed functional enrichment analysis on the top 200 spatially coexpressed genes. Functional enrichment analysis was performed using Enrichr (40). For each region, we report the top 10 enriched Gene Ontology biological process and molecular function.

Gene Set Analysis. To assess the coexpression between a set of genes and a steroid receptor of interest, a Mann–Whitney U test is used. The test assesses the null hypothesis that the correlations of the set of targets or mediators, on the one hand, and the correlations of all other genes, on the other hand, are independent samples from identical continuous distributions with equal medians, against the alternative that they do not have equal medians. The returned P values from different experiments are corrected for multiple testing by controlling the FDR using the Benjamini–Hochberg method (41) (FDR-corrected).

Selecting Targets for Validation. To select genes for validation, we generated a list of genes ranked by the strength of their coexpression with *Esr1* in the HY. We restricted our analysis to the list of genes with a coronal experiment in the ABA (4,345 genes; Dataset S5). To improve our predictions of coexpressed genes, we filtered out genes with a normalized average expression $<T_{HY}$ in the HY. In our experiments, we used $T_{HY} = 0.5$ because the average expression of our receptor of interest, *Esr1*, in the HY was 0.44. After filtering, we selected the top 10 coexpressed genes as *Esr1*-related genes for validation using qPCR. In contrast, we selected the 10 genes showing the weakest coexpression with *Esr1* (correlation ≈ 0) as a background set.

Sum of Ranks Analysis. To assess a set of coexpressed genes for a seed gene in a set of functionally related brain structures, such as the dopaminergic system composed of the VTA and SN (Fig. S1), we used a rank sum analysis. We ranked all genes based on their correlation to the seed gene within the structure of interest. Because the number of samples (voxels) used in the correlation calculation varies between different brain structures (i.e., brain structures have different numbers of voxels), comparisons of coexpression across different structures are carried out based on the rank of the gene in a specific list rather than by comparing correlation values. Given a set of structures S , we calculate the sum of ranks RS such that: $RS_{ij}^S = \sum_{s \in S} R_{ij}^s$, where R_{ij}^s is the rank of the correlation between gene i and gene j in structure s . The rank of the correlation is calculated as the rank of the correlation

value between seed gene i and target gene j among the list of correlations of all genes with the seed gene i .

We assessed the significance of the sum of ranks value based on permutations. Given a set of n functionally related brain structures, we randomly draw n random integers from a discrete uniform distribution ranging from 1 to the total number of genes (26,022 in the case of all genes and 4,345 in the case of genes with coronal-only experiment). We repeated the experiment 10,000 times and calculated the sum of the randomly drawn numbers to obtain a probability distribution function of obtaining a certain sum of ranks.

Validation Using qPCR and dISH. C57BL/6J mice were obtained from Charles River Laboratories at the indicated age and were kept for 1 wk under standard housing conditions before they were enrolled in an experimental setup. Nine-week-old male mice underwent gonadectomy or a sham operation under isoflurane anesthesia. Gonadectomy involved a small incision in the skin after which the testes were removed. After 1 wk of recovery, these mice received daily s.c. injections with 100 μ g/kg DES (Steraloids, Inc.) dissolved in olive oil or the olive oil vehicle alone for 1 wk before they were terminated by cardiac puncture under isoflurane anesthesia. Brains were rapidly dissected and frozen on powdered dry ice, and stored at -80°C . All animal experiments were performed with the approval of the Animal Ethics Committee at Erasmus Medical Center. To collect mRNA, frozen brains were cut sagittally over the midline, and 60- μm sections containing HY from one hemisphere were collected on uncoated glass slides (Menzel–Gläser). Hypothalamic tissue was punched out using appropriate Harris Uni-core punching needles (Tedpella)

and pooled per anterior (+0.26 to -1.22 mm relative to bregma) or posterior (-1.22 to -2.7 mm relative to bregma) division. RNA isolation and cDNA synthesis have been performed as described in ref. 42. qPCR was performed on a IQ5 PCR platform (Bio-Rad) as described by Boon et al. (43), using 36b4 as a housekeeping gene. Primer sequences are listed in Dataset S6.

For nonisotopic double-label semiquantitative ISH, we used the Panomics View-RNA method (Affymetrix). Probe sets were designed by, and are available from, the manufacturer. Twelve-micrometer-thick section cryosections on Superfrost Plus microscope slides (Menzel Gläser) were postfixed in 4% (vol/vol) formaldehyde (Sigma–Aldrich). Preincubation was performed following the manufacturer's instructions (<https://www.panomics.com/>). Probes were hybridized for 4 h in a Startspin thermobrite stove (Iris Sample Processing). Linear amplification and visualization steps were performed following the manufacturer's instructions. Slides were lightly counterstained with Mayer's hematoxylin and DAPI (1 min of incubation at 3 $\mu\text{g}/\text{mL}$), and embedded in Innovex mounting medium (Innovex Biosciences).

Validation Using ChIP-Seq. We remapped the ChIP-Seq data from Polman et al. (28) to the *Rattus Norvegicus* genome version 5 (rn5) using the Burrow–Wheeler Aligner (44) on default settings. GR peaks were called using model-based analysis of ChIP-Seq (MACS) (45), version 2.14, with the IgG Ab-binding dataset as the background using the following settings: P value cutoff = 0.05; model fold = [10, 40]; λ = 1,000/10,000; effective genome size = 2.5×10^9 . In total, we identified 694 genes with intergenic GR binding peaks. Data were visualized by uploading bigwig files to the Integrative Genomics Viewer (IGV) (46).



Fig. S1. Dopaminergic system in the mouse brain. A coronal section from the Allen Brain Atlas (4) shows the VTA and SN (thick black contour) that composes the dopaminergic system, indicated.

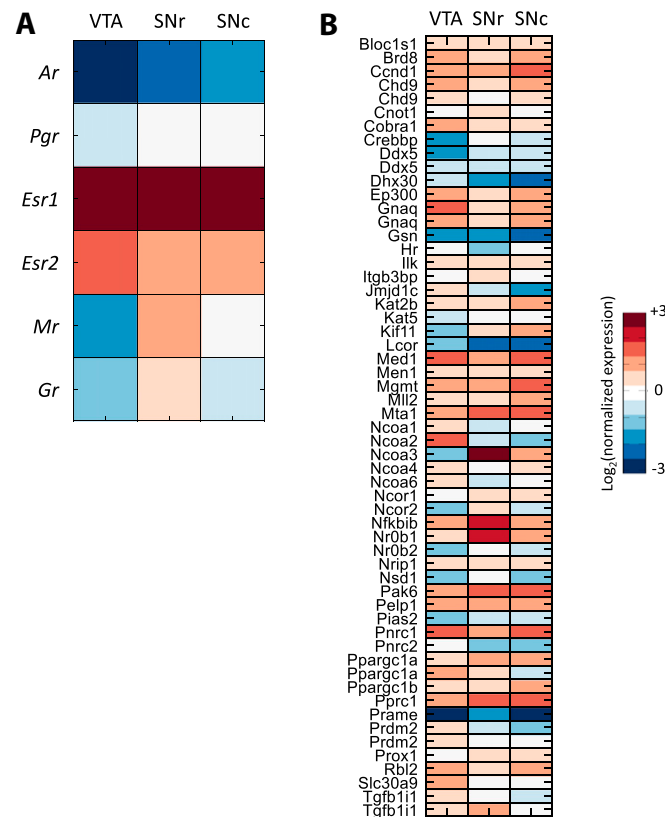


Fig. S2. Expression of steroid receptors and coregulators in the dopaminergic system. The expression of six steroid receptors (*A*) and 62 coregulators (*B*) in the VTA, SN reticular part (SNr), and SN compact part (SNC). Reported values are the average expression energy per region normalized to the average expression across the whole brain and then log₂-transformed.

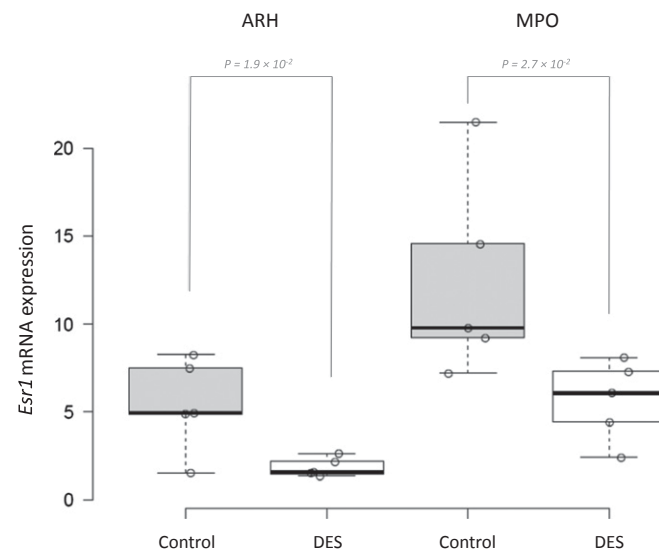


Fig. S3. Down-regulation of mRNA levels of *Esr1* in response to DES treatment. The mRNA levels of *Esr1*, measured using dISH, were significantly down-regulated ($P < 0.05$) in the anterior (MPO) and posterior (ARH) HY of the control and DES-treated mice.

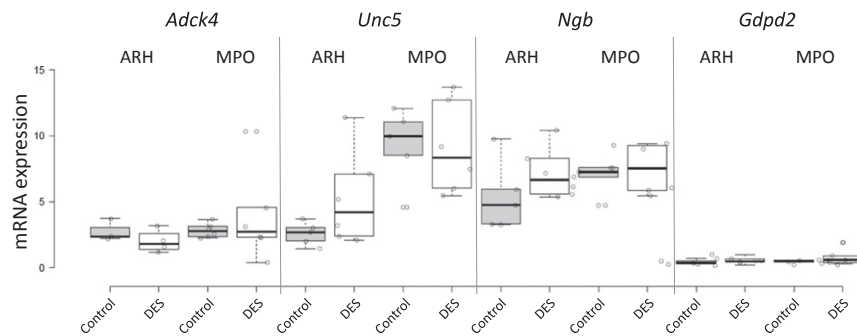


Fig. S4. Response of *Esr1*-coexpressed genes to DES treatment. The mRNA levels of *Adck4*, *Unc5*, *Ngb*, and *Gdpd2* were measured using dISH in the anterior (MPO) and posterior (ARH) HY of the control and DES-treated mice.

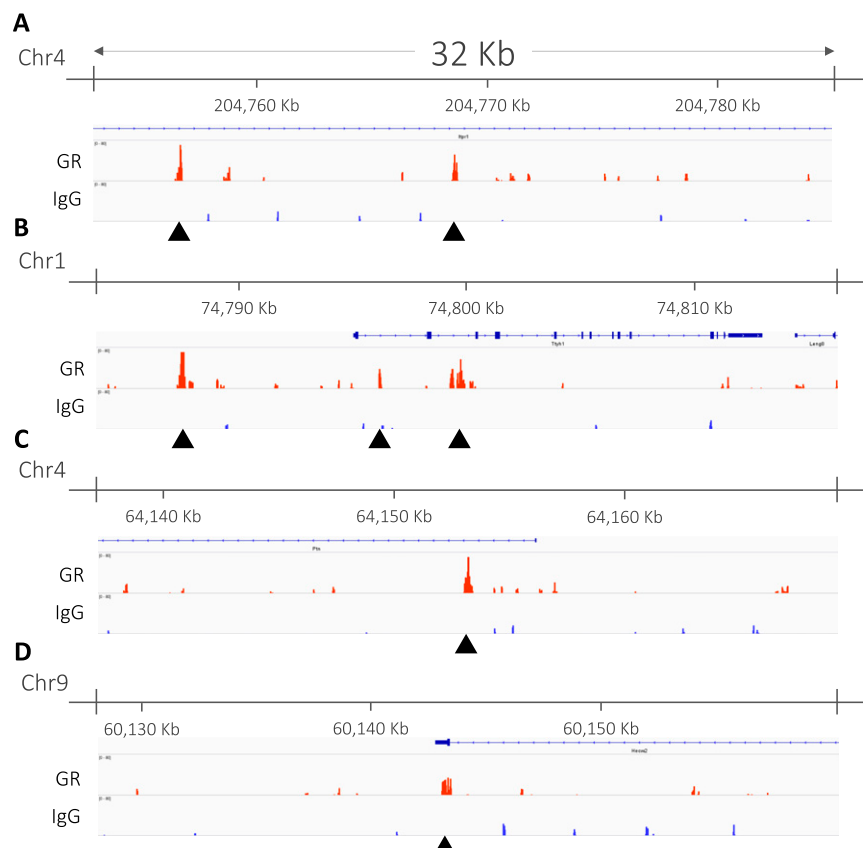


Fig. S5. Validating GR targets in hippocampus using ChIP-Seq. Examples of GR binding sites to genes strongly coexpressed with *Gr* in the hippocampus: *Itp1* (A), *Ttyh1* (B), *Ptn* (C), and *Hecw2* (D). For each gene, a genomic region of 32 kb centered around the identified peak is shown using the Integrative Genomics Viewer (46). Black arrows indicate the intergenic peaks identified within the gene.

Table S1. Gene ontology enrichment of the top 200 genes correlated with *Esr1* and *Gr* in 12 brain regions

[Table S1](#)

Table S2. Coexpression of sexually dimorphic genes with *Esr1* (coronal experiment) in the whole brain

[Table S2](#)

Table S3. Response of *Ers1*-coexpressed and non-coexpressed genes to DES treatment in the anterior and posterior HY

[Table S3](#)

Table S4. GR targets in the hippocampus validated by ChIP-Seq

[Table S4](#)

Table S1: Gene Ontology enrichment of the top 200 genes correlated with *Esr1* and *Gr* in 12 brain regions.

	<i>Esr1</i>		<i>Gr</i>	
	Term	P-value	Term	P-value
Cerebellum (CB)	synaptic transmission (GO:0007268)	5.08E-05	regulation of receptor internalization (GO:0002090)	4.39E-03
	regulation of membrane potential (GO:0042391)	1.20E-04	glucose catabolic process (GO:0006007)	1.48E-02
	calcium ion import (GO:0070509)	4.63E-04	sympathetic nervous system development (GO:0048485)	1.48E-02
	regulation of type 2 immune response (GO:0002828)	2.23E-03	regulation of early endosome to late endosome transport (GO:2000641)	7.78E-03
	single-organism behavior (GO:0044708)	1.46E-03	intracellular protein transmembrane transport (GO:0065002)	5.67E-03
	neuropeptide hormone activity (GO:0005184)	2.25E-03	RNA polymerase II transcription corepressor activity (GO:0001106)	2.20E-03
	neuropeptide receptor binding (GO:0071855)	3.09E-03	ATPase activator activity (GO:0001671)	1.03E-02
	peptidase activator activity (GO:0016504)	7.71E-03	heparan sulfate sulfotransferase activity (GO:0034483)	1.03E-02
	gated channel activity (GO:0022836)	6.79E-03	transcription corepressor activity (GO:0003714)	4.96E-03
	hormone activity (GO:0005179)	1.94E-03	insulin-like growth factor receptor binding (GO:0005159)	1.16E-02
Cortical subplate (CTXsp)	regulation of hormone levels (GO:0010817)	1.15E-04	alkali metal ion binding (GO:0031420)	8.09E-03
	pattern specification process (GO:0007389)	7.26E-05	potassium ion binding (GO:0030955)	4.34E-03
	regionalization (GO:0003002)	1.99E-04	death receptor activity (GO:0005035)	6.09E-03
	neurogenesis (GO:0022008)	3.64E-04	prenyltransferase activity (GO:0004659)	1.04E-02
	negative regulation of embryonic development (GO:0045992)	1.24E-03	MAP kinase activity (GO:0004707)	9.20E-03
	RNA polymerase II core promoter proximal region sequence-specific DNA binding transcription factor activity (GO:0000982)	1.36E-03	peroxisomal transport (GO:0043574)	8.18E-04
	receptor antagonist activity (GO:0048019)	4.51E-03	protein localization to peroxisome (GO:0072662)	1.21E-02
	receptor inhibitor activity (GO:0030547)	5.23E-03	protein targeting to peroxisome (GO:0006625)	1.21E-02
	neurotransmitter binding (GO:0042165)	9.58E-03	membrane hyperpolarization (GO:0060081)	2.22E-03
	excitatory extracellular ligand-gated ion channel activity (GO:0005231)	7.46E-03	aerobic respiration (GO:0009060)	2.10E-02
Hippocampal formation (HDF)	uterus development (GO:0060065)	5.96E-06	calcium channel regulator activity (GO:0005246)	3.30E-04
	maternal process involved in female pregnancy (GO:0060135)	1.82E-04	MAP kinase phosphatase activity (GO:0033549)	7.37E-04
	polyol catabolic process (GO:0046174)	9.22E-03	channel regulator activity (GO:0016247)	5.82E-04
	dopaminergic neuron differentiation (GO:0071542)	5.94E-03	receptor signaling protein activity (GO:0005057)	2.56E-04
	regulation of hair cycle (GO:0042634)	1.01E-02	substrate-specific channel activity (GO:0022838)	2.15E-03
	plus-end-directed microtubule motor	7.04E-03	single-organism behavior (GO:0044708)	1.87E-06

	activity (GO:0008574)			
	neurotransmitter:sodium symporter activity (GO:0005328)	8.57E-03	gamma-aminobutyric acid signaling pathway (GO:0007214)	1.07E-05
	immunoglobulin binding (GO:0019865)	1.11E-02	regulation of synaptic transmission (GO:0050804)	1.46E-05
	neurotransmitter transporter activity (GO:0005326)	1.30E-02	behavior (GO:0007610)	2.14E-05
	hyaluronic acid binding (GO:0005540)	1.11E-02	cognition (GO:0050890)	7.02E-06
Hypothalamus (HY)	feeding behavior (GO:0007631)	1.31E-04	regulation of oligodendrocyte differentiation (GO:0048713)	1.31E-03
	pigment cell differentiation (GO:0050931)	1.47E-03	circadian behavior (GO:0048512)	1.91E-03
	melanocyte differentiation (GO:0030318)	1.17E-03	rhythmic behavior (GO:0007622)	2.27E-03
	insulin-like growth factor receptor signaling pathway (GO:0048009)	7.80E-03	positive regulation of glial cell differentiation (GO:0045687)	1.31E-03
	adult feeding behavior (GO:0008343)	4.38E-03	positive regulation of mesenchymal cell proliferation (GO:0002053)	2.47E-04
	peptide hormone binding (GO:0017046)	3.63E-03	cysteine-type endopeptidase inhibitor activity involved in apoptotic process (GO:0043027)	4.82E-04
	insulin receptor binding (GO:0005158)	3.35E-03	acid phosphatase activity (GO:0003993)	3.92E-03
	ligand-gated ion channel activity (GO:0015276)	1.95E-03	cysteine-type endopeptidase regulator activity involved in apoptotic process (GO:0043028)	2.85E-03
	ligand-gated channel activity (GO:0022834)	1.95E-03	glycoprotein binding (GO:0001948)	2.62E-03
	growth factor binding (GO:0019838)	4.99E-03	heparan sulfate proteoglycan binding (GO:0043395)	7.20E-03
Isocortex	monoamine transport (GO:0015844)	8.19E-04	negative regulation of phosphorylation (GO:0042326)	3.32E-07
	positive regulation of myeloid leukocyte cytokine production involved in immune response (GO:0061081)	4.06E-03	negative regulation of phosphorus metabolic process (GO:0010563)	3.11E-07
	oocyte development (GO:0048599)	5.41E-03	negative regulation of protein kinase activity (GO:0006469)	8.72E-07
	central nervous system neuron development (GO:0021954)	1.86E-03	negative regulation of kinase activity (GO:0033673)	1.69E-06
	type B pancreatic cell development (GO:0003323)	4.06E-03	negative regulation of protein phosphorylation (GO:0001933)	3.80E-06
	immunoglobulin binding (GO:0019865)	8.76E-04	phosphoric ester hydrolase activity (GO:0042578)	4.04E-05
	hydrolase activity, hydrolyzing N-glycosyl compounds (GO:0016799)	1.42E-02	phosphoprotein phosphatase activity (GO:0004721)	2.25E-05
	dicarboxylic acid transmembrane transporter activity (GO:0005310)	1.66E-02	MAP kinase phosphatase activity (GO:0033549)	9.84E-04
	MAP kinase activity (GO:0004707)	6.44E-03	Hsp70 protein binding (GO:0030544)	2.23E-03
	sodium channel regulator activity (GO:0017080)	2.04E-02	phosphatase activity (GO:0016791)	6.84E-04
Midbrain (MBR)	H4 histone acetyltransferase activity (GO:0010485)	6.86E-04	regulation of postsynaptic membrane potential (GO:0060078)	1.48E-07
	neurotransmitter transporter activity (GO:0005326)	2.30E-03	regulation of dendritic spine morphogenesis (GO:0061001)	3.39E-06
	cofactor binding (GO:0048037)	1.60E-03	regulation of membrane potential	1.70E-06

	structural constituent of ribosome (GO:0003735)	1.32E-03	(GO:0042391) regulation of excitatory postsynaptic membrane potential (GO:0060079)	1.07E-06
	peptide hormone binding (GO:0017046)	5.27E-03	positive regulation of excitatory postsynaptic membrane potential (GO:2000463)	4.35E-05
	cholesterol biosynthetic process (GO:0006695)	5.50E-09	ephrin receptor binding (GO:0046875)	9.17E-07
	sterol biosynthetic process (GO:0016126)	1.41E-08	metal ion transmembrane transporter activity (GO:0046873)	3.64E-04
	organic hydroxy compound biosynthetic process (GO:1901617)	1.13E-06	kinase binding (GO:0019900)	6.07E-04
	organic hydroxy compound metabolic process (GO:1901615)	2.13E-05	potassium ion transmembrane transporter activity (GO:0015079)	3.52E-04
	isoprenoid biosynthetic process (GO:0008299)	1.23E-04	gated channel activity (GO:0022836)	9.05E-04
Medulla (M)	learning or memory (GO:0007611)	3.62E-08	oxidoreductase activity, acting on a sulfur group of donors, NAD(P) as acceptor (GO:0016668)	4.21E-03
	cognition (GO:0050890)	1.64E-07	transforming growth factor beta receptor binding (GO:0005160)	1.65E-02
	regulation of synaptic transmission (GO:0050804)	2.40E-06	enzyme activator activity (GO:0008047)	4.35E-03
	memory (GO:0007613)	2.12E-06	protein homodimerization activity (GO:0042803)	3.22E-03
	single-organism behavior (GO:0044708)	2.28E-05	RNA polymerase II distal enhancer sequence-specific DNA binding transcription factor activity involved in positive regulation of transcription (GO:0001205)	1.78E-02
	protein kinase C activity (GO:0004697)	6.70E-04	serine family amino acid catabolic process (GO:0009071)	3.45E-04
	clathrin binding (GO:0030276)	3.31E-02	L-serine metabolic process (GO:0006563)	8.68E-05
	HMG box domain binding (GO:0071837)	1.44E-02	response to reactive oxygen species (GO:0000302)	2.27E-04
	neurotransmitter:sodium symporter activity (GO:0005328)	1.59E-02	excretion (GO:0007588)	7.08E-04
	semaphorin receptor binding (GO:0030215)	5.26E-03	placenta development (GO:0001890)	4.06E-03
Olfactory areas (OLF)	T cell mediated immunity (GO:0002456)	1.12E-03	phosphatidylinositol dephosphorylation (GO:0046856)	1.21E-03
	alpha-beta T cell differentiation involved in immune response (GO:0002293)	7.33E-04	inactivation of MAPK activity (GO:0000188)	5.19E-04
	T cell differentiation involved in immune response (GO:0002292)	7.33E-04	negative regulation of protein modification process (GO:0031400)	6.09E-04
	alpha-beta T cell activation involved in immune response (GO:0002287)	7.33E-04	negative regulation of protein phosphorylation (GO:0001933)	6.80E-04
	G-protein coupled receptor signaling pathway, coupled to cyclic nucleotide second messenger (GO:0007187)	1.05E-04	negative regulation of transferase activity (GO:0051348)	1.30E-03
	heparan sulfate proteoglycan binding (GO:0043395)	5.76E-04	MAP kinase phosphatase activity (GO:0033549)	1.00E-03
	proteoglycan binding (GO:0043394)	1.93E-03	phosphatase activity (GO:0016791)	7.24E-04

	excitatory extracellular ligand-gated ion channel activity (GO:0005231)	9.02E-04	protein tyrosine phosphatase activity (GO:0004725)	1.07E-03
	neurotransmitter receptor activity (GO:0030594)	5.02E-04	calcium-dependent protein binding (GO:0048306)	4.65E-04
	protein phosphatase binding (GO:0019903)	1.40E-03	phosphoric ester hydrolase activity (GO:0042578)	2.01E-03
Pons (P)	cell-cell adhesion (GO:0098609)	4.17E-07	positive regulation of cardiac muscle hypertrophy (GO:0010613)	4.86E-04
	cell-cell adhesion via plasma-membrane adhesion molecules (GO:0098742)	3.96E-07	positive regulation of muscle hypertrophy (GO:0014742)	4.86E-04
	homophilic cell adhesion via plasma membrane adhesion molecules (GO:0007156)	1.52E-06	positive regulation of cellular component movement (GO:0051272)	3.57E-04
	heterophilic cell-cell adhesion via plasma membrane cell adhesion molecules (GO:0007157)	3.35E-04	positive regulation of locomotion (GO:0040017)	4.38E-04
	regulation of cell adhesion (GO:0030155)	3.98E-04	pigmentation (GO:0043473)	4.42E-04
	excitatory extracellular ligand-gated ion channel activity (GO:0005231)	1.46E-03	cGMP binding (GO:0030553)	2.91E-05
	extracellular ligand-gated ion channel activity (GO:0005230)	9.06E-04	RAGE receptor binding (GO:0050786)	2.18E-04
	extracellular-glutamate-gated ion channel activity (GO:0005234)	1.51E-02	cyclic nucleotide binding (GO:0030551)	3.91E-04
	ionotropic glutamate receptor activity (GO:0004970)	1.66E-02	sodium:dicarboxylate symporter activity (GO:0017153)	4.68E-03
	hexosaminidase activity (GO:0015929)	1.10E-02	calcium ion binding (GO:0005509)	3.48E-03
Palladium (PAL)	toxin metabolic process (GO:0009404)	1.71E-04	2-oxoglutarate metabolic process (GO:0006103)	5.47E-04
	synaptic transmission (GO:0007268)	2.72E-05	regulation of steroid hormone biosynthetic process (GO:0090030)	3.89E-04
	response to steroid hormone (GO:0048545)	1.22E-04	multicellular organismal aging (GO:0010259)	5.47E-04
	positive regulation of secretion (GO:0051047)	4.89E-05	brown fat cell differentiation (GO:0050873)	2.50E-04
	behavior (GO:0007610)	9.85E-05	steroid metabolic process (GO:0008202)	3.03E-04
	neuropeptide hormone activity (GO:0005184)	8.81E-08	endodeoxyribonuclease activity, producing 5'-phosphomonoesters (GO:0016888)	1.02E-02
	GABA-A receptor activity (GO:0004890)	1.07E-06	GTPase activating protein binding (GO:0032794)	7.96E-03
	GABA receptor activity (GO:0016917)	2.00E-06	anion:anion antiporter activity (GO:0015301)	2.31E-02
	hormone activity (GO:0005179)	8.71E-06	receptor signaling complex scaffold activity (GO:0030159)	1.54E-02
	extracellular ligand-gated ion channel activity (GO:0005230)	4.02E-05	cysteine-type endopeptidase inhibitor activity involved in apoptotic process (GO:0043027)	1.68E-02
Striatum (STR)	CD4-positive, alpha-beta T cell differentiation (GO:0043367)	1.13E-04	synaptic transmission (GO:0007268)	1.12E-07
	epithelial cell maturation (GO:0002070)	7.15E-04	potassium ion transmembrane transport (GO:0071805)	4.08E-06
	T-helper cell differentiation (GO:0042093)	6.06E-04	cellular potassium ion transport (GO:0071804)	4.08E-06
	alpha-beta T cell differentiation involved in immune response (GO:0002293)	8.35E-04	potassium ion transport (GO:0006813)	1.36E-05

	neuron projection guidance (GO:0097485)	2.51E-04	regulation of ion transmembrane transport (GO:0034765) potassium ion transmembrane transporter activity (GO:0015079)	1.63E-04
	ligand-activated sequence-specific DNA binding RNA polymerase II transcription factor activity (GO:0004879)	1.38E-04		6.99E-06
	steroid hormone receptor activity (GO:0003707)	2.44E-04	potassium channel activity (GO:0005267)	1.77E-05
	14-3-3 protein binding (GO:0071889)	8.64E-04	voltage-gated potassium channel activity (GO:0005249)	2.01E-05
	chloride channel activity (GO:0005254)	6.68E-04	inward rectifier potassium channel activity (GO:0005242)	8.04E-05
	anion channel activity (GO:0005253)	1.05E-03	monovalent inorganic cation transmembrane transporter activity (GO:0015077)	3.48E-04
Thalamus (TH)	synaptic transmission (GO:0007268)	3.17E-06	regulation of transmembrane transporter activity (GO:0022898)	3.10E-06
	chloride transmembrane transport (GO:1902476)	8.57E-06	regulation of ion transmembrane transporter activity (GO:0032412)	2.43E-06
	chloride transport (GO:0006821)	1.50E-05	regulation of transporter activity (GO:0032409)	6.15E-06
	nephron epithelium morphogenesis (GO:0072088)	1.74E-04	regulation of metal ion transport (GO:0010959)	1.44E-05
	nephron tubule morphogenesis (GO:0072078)	1.74E-04	regulation of ion transmembrane transport (GO:0034765)	2.82E-05
	extracellular ligand-gated ion channel activity (GO:0005230)	3.15E-08	quaternary ammonium group binding (GO:0050997)	4.82E-04
	ligand-gated ion channel activity (GO:0015276)	7.41E-07	steroid hormone receptor activity (GO:0003707)	4.85E-04
	ligand-gated channel activity (GO:0022834)	7.41E-07	SMAD binding (GO:0046332)	1.03E-03
	excitatory extracellular ligand-gated ion channel activity (GO:0005231)	5.99E-06	phospholipid binding (GO:0005543)	1.50E-03
	chloride transmembrane transporter activity (GO:0015108)	1.35E-05	ephrin receptor binding (GO:0046875)	5.41E-03

Table S2: Coexpression of sexually dimorphic genes with *Esr1* (coronal experiment) in the whole brain.

Gene	Whole Brain				Hypothalamus				
	Gene	Correlation	Correlation Rank	Expression*	Expression Rank	Correlation	Correlation Rank	Expression\$	Expression Rank
<i>Irs4</i>		0.51	1	0.41	14362	0.82	1	7.24	14
<i>Pak3</i>		0.39	9	1.26	9650	0.54	64	1.73	990
<i>Gpr165</i>		0.39	10	1.60	8662	0.55	48	5.09	50
<i>Ecel1</i>		0.36	17	2.25	7303	0.41	404	4.72	60
<i>Glra3</i>		0.26	87	0.60	12639	0.48	159	2.75	251
<i>Gabrg1</i>		0.26	89	0.79	11511	0.29	1467	2.59	315
<i>Nnat</i>		0.24	123	6.42	3277	0.29	1609	2.33	431
<i>Cartpt</i>		0.23	160	0.80	11467	0.18	3716	3.04	210
<i>Greb1</i>		0.17	452	0.36	14918	0.41	414	1.13	3427
<i>Rps6ka6</i>		0.16	480	0.78	11575	0.41	418	1.30	2189
<i>Sytl4</i>		0.16	513	0.18	18245	0.49	128	1.60	1194
<i>Brs3</i>		0.11	1313	0.23	17160	0.48	141	1.19	2871
<i>Cckar</i>		0.10	1555	1.37	9300	-0.09	17153	0.96	5518
<i>Dgkk</i>		-0.02	15812	1.52	8884	0.11	5828	0.67	11142
<i>Chodl</i>		-0.05	20934	0.25	16690	-0.15	21688	0.56	13760

* Average expression across all brain voxels.

\$ Average expression across all hypothalamus voxels, normalized by the average expression across the whole brain.

Table S3: Response of *Ers1*-coexpressed and noncoexpressed genes to DES treatment in the anterior and posterior hypothalamus.

Gene	Correlation	Correlation Rank	Expression*	Expression Rank	Anterior HY (fold change)	Anterior HY (p-value)	Posterior HY (fold change)	Posterior HY (p-value)
Irs4	0.79	1	7.24	1	1.45	0.04	1.26	0.19
Fut8	0.75	2	0.36	3367	1.10	0.32	1.34	0.23
Gdpd2	0.66	4	3.54	42	1.34	0.04	1.08	0.24
Ngb	0.64	6	6.24	8	1.44	0.05	1.24	0.21
Rfx7	0.63	7	0.98	1195	1.16	0.24	1.08	0.14
Adck4	0.62	8	1.98	141	1.31	0.05	1.30	0.09
Ltbp4	0.60	9	1.13	737	1.20	0.12	0.87	0.14
Magel2	0.57	11	5.63	11	1.47	0.06	1.25	0.18
Unc5d	0.57	13	1.52	284	1.32	0.10	1.34	0.08
Bhlhb9	0.57	15	0.62	2473	1.17	0.11	1.02	0.39
Mtss1	4.40E-05	2237	0.70	2231	1.21	0.17	1.18	0.01
Ern2	1.96E-04	2235	0.40	3210	1.70	0.01	1.18	0.20
Olig2	3.04E-04	2234	0.83	1722	1.12	0.23	0.88	0.25
Pip5k1c	3.94E-04	2232	0.73	2119	1.15	0.22	1.01	0.46
Megf11	7.35E-04	2230	0.34	3423	1.27	0.04	0.91	0.17
Chat	7.96E-04	2229	1.33	423	1.36	0.20	1.12	0.40
Ltb	8.01E-04	2228	0.24	3787	1.18	0.19	0.95	0.39
Gnas	9.13E-04	2227	1.10	803	1.33	0.04	0.92	0.20
Tmem150c	1.07E-03	2225	0.76	1992	1.27	0.10	0.90	0.16
Cyb5r1	1.52E-03	2223	0.82	1778	1.20	0.15	1.11	0.22

* Average expression across all hypothalamus voxels, normalized by the average expression across the whole brain.

Table S4: GR targets in the hippocampus validated by CHIP-seq.

	Gene symbol	Correlation Rank	Correlation	chr	start	end	-LOG10(q-value)
1	Itpr1	4	0.78	chr4	204768526	204768670	12.56
2	Ttyh1	8	0.77	chr1	74799541	74799835	10.49
3	Ptn	26	0.72	chr4	64153042	64153257	21.54
4	Hecw2	28	0.72	chr9	60143115	60143327	6.48
5	RGD1306534	31	0.71	chr3	169558683	169558795	6.52
6	Ntrk2	36	0.70	chr17	8206110	8206216	10.50
7	Hivep1	62	0.68	chr17	24367329	24367491	5.24
8	Rab11fip4	69	0.67	chr10	64629571	64629807	25.34
9	Arntl	71	0.67	chr1	185027529	185027725	22.82
10	Galnt9	74	0.67	chr12	53884426	53884529	8.48
11	Plcl2	78	0.66	chr9	1764414	1764522	10.50
12	RGD1560050	115	0.64	chr15	108459125	108459244	8.48
13	RGD1305961	117	0.64	chr6	50704731	50704884	48.69
14	Sdk2	131	0.63	chr10	101994116	101994399	10.50
15	Fhod3	176	0.61	chr18	16990799	16990917	10.50
16	Dcip2	180	0.61	chr9	18406124	18406371	46.11